

A Preliminary in Silico Lead Series of 2-Phthalimidinoglutamic Acid Analogues Designed as MMP-3 Inhibitors

Elizabeth A. Amin[†] and William J. Welsh[‡]

Department of Chemistry and Minnesota Supercomputing Institute, University of Minnesota,
207 Pleasant St SE, Minneapolis, Minnesota 55455, and Department of Pharmacology,
Robert Wood Johnson Medical School—University of Medicine and Dentistry of New Jersey,
675 Hoes Lane, Piscataway, New Jersey 08854

Received April 12, 2006

Matrix metalloproteinases (MMPs) have been the subject of intense research because of their roles in tumor metastasis and in the rise and spread of degenerative diseases such as osteo- and rheumatoid arthritis. A preliminary class of 140 druglike, small-molecule matrix metalloproteinase-3 inhibitors, intended as starting scaffolds for optimization and synthesis, has been designed in silico using a series of highly predictive three-dimensional quantitative structure–activity relationship models, including comparative molecular field analysis and comparative molecular similarity indices analysis, with docking and scoring. Thalidomide was chosen as the skeleton on which to base the new lead series, as it moderately inhibits MMP-3, is antiangiogenic, and lends itself easily to structural modifications. Most of the new compounds demonstrate medium to high predicted biological activity and good bioavailability as estimated by the octanol–water partition coefficient ClogP. Compound 102 in particular exhibits extremely favorable predicted activity against MMP-3; is moderately bioavailable; satisfies Lipinski's Rule of Five; and shows promise for further optimization, synthesis, and experimental evaluation as a potential adjunct anticancer or antirheumatic therapeutic.

INTRODUCTION

Matrix metalloproteinases (MMPs) comprise a class of approximately 23 structurally related, zinc-binding enzymes that mediate the breakdown of extracellular matrix proteins (EMPs) such as collagens, elastin, and gelatin.^{1–4} While MMPs play crucial roles in many beneficial tissue remodeling functions such as wound healing and cartilage turnover, their aberrant expression contributes to many diseases marked by uncontrolled matrix degradation, inflammation, and excessive tissue destruction.^{5,6} MMPs have been identified in tissue surrounding invasive carcinoma^{7,8} and have been linked to progressive structural joint degradation in osteo- and rheumatoid arthritis.^{9–11} They directly enable tumor metastasis through angiogenesis-related EMP breakdown.^{12–15} These enzymes have therefore become attractive targets for small-molecule synthetic inhibitors (MMPIs) that would serve as adjunct antitumor and antiarthritic therapeutic agents. MMP-3 (stromelysin-1) in particular has been found in the vicinity of melanomas and other metastatic tumors.^{16,17} MMP-3 has been shown to hydrolyze several key extracellular matrix proteins comprising more than 70% of human cartilage and is an active precursor to the action of other endopeptidases.^{18,19} However, the success of MMPIs in clinical trials has been limited by bioavailability and toxicity issues, roadblocks that can partly be addressed by means of recent advances in computer-aided drug design such as those applied in this study.

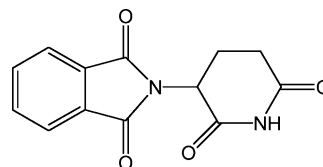


Figure 1. Thalidomide.

We have applied a series of validated, highly predictive three-dimensional quantitative structure–activity relationship (3D-QSAR) models to design a preliminary lead series of bioavailable MMP-3 inhibitors with favorable predicted absorption, distribution, metabolism, excretion, and toxicity (ADME/Tox) properties that stand ready for synthesis, optimization, and experimental binding assays. The structures are based on a modified thalidomide (2-phthalimidinoglutamic acid) skeleton, as thalidomide exhibits a wide range of biological activity, is antineoplastic, and is considered to influence various growth factors as well as boost the immune response,^{20,21} all of which render it a promising anticancer drug on its own. While thalidomide (Figure 1) is notorious for having caused birth defects in the 1950s when taken by pregnant women to relieve nausea, it is currently experiencing a resurgence in popularity among researchers because of its strong, broad-spectrum activity against a variety of malignant autoimmune and degenerative diseases.²² Thalidomide has been successfully used against erythema nodosum leprosum²³ and downregulates tumor necrosis factor alpha (TNF- α), a molecule directly involved in autoimmune diseases, the general immune response, and cancer.^{24,25} There is, however, a poor correlation between TNF- α activity and antitumor activity.²⁶ Most notably, thalidomide functions as a potent angiogenesis inhibitor, retarding the growth of new

* Corresponding author phone: 612-626-2387; fax: 612-626-7541; e-mail: amin@chem.umn.edu.

[†] University of Minnesota.

[‡] Robert Wood Johnson Medical School—University of Medicine and Dentistry of New Jersey.

blood vessels in malignant tumors and other rapidly proliferating tissues^{27,28}—a process in which MMPs are intimately involved.

The thalidomide molecule lends itself readily to structural and pharmacophoric modifications. Two successful classes of molecules have been derived from thalidomide: selective cytokine inhibitors targeting phosphodiesterase type 4 and immunomodulatory drugs (IMiDs)²² that show strong anti-angiogenic and T-cell costimulatory abilities. Lenalidomide, the primary second-generation IMiD, has demonstrated clinical benefits in both myelodysplastic syndrome and multiple myeloma, with no evidence of teratogenicity²⁹ and a more favorable safety profile than thalidomide. Additionally, Green and co-workers have successfully synthesized and evaluated a series of modified thalidomide analogues designed as antitumor agents and have identified structural features that enhance *in vivo* antitumor activity,³⁰ although the mechanism of this activity is not yet known. These and other studies^{31,26} suggest that the thalidomide molecule can be modified to filter out dangerous side effects while retaining or enhancing specific biological activity—a valuable starting point for MMPI design and optimization.

METHODOLOGY

All calculations and visualizations described herein were performed on Silicon Graphics O2 workstations running under the IRIX 6.5 operating system and on an Alienware MJ-12 dual-CPU workstation running under the SuSE Linux Professional 9.3 OS. 3D-QSAR models and docking/scoring were performed in the SYBYL 6.7 and SYBYL 7.0 molecular modeling software packages.³²

3D-QSAR Training Series. We have developed highly predictive 3D-QSAR models using comparative molecular field analysis (CoMFA)³³ and comparative molecular similarity indices analysis (CoMSIA)³⁴ for three series of MMPIs: (1) 39 piperazine-based compounds derived from *dl*-piperazinecarboxylic acid (TS 1),³⁵ (2) 39 arylsulfonyl isoquinoline derivatives (TS 2),³⁶ and (3) 35 thiazine- and thiazepine-based ligands (TS 3).³⁷ These models are distinguished by their high self-consistency and internal predictivity and are published elsewhere.^{38,39} 3D-QSAR requires no initial active-site information and can therefore be used to elucidate a wide variety of enzyme–inhibitor interactions for which, as in the case of the present work, reliable force-field parameters for bound metals are not easily obtainable. Rather than computing ligand–receptor binding energies (a nontrivial task for metal-binding enzymes such as MMPs), these methods sample steric and electrostatic fields (CoMFA) or calculate similarity indices (CoMSIA) surrounding an established compound set and then correlate differences in those fields or indices with experimental biological activity. Both CoMFA and CoMSIA have been shown in multiple studies^{40–43} to be powerful and effective techniques for designing novel ligands, improving the potency of existing inhibitors, mapping previously unmodeled active-site properties, and clarifying mechanisms of action.

It is important to note that predictions of biological activity by CoMFA and CoMSIA models are strongly dependent on structural similarity between the compounds being evaluated and those used to generate the model. To predict the activities of a thalidomide-based lead series, the preferred 3D-QSAR

training set(s) would comprise thalidomide-based MMPIs with consistent, reliable experimental activity data. However, such data have not yet been published, so the TS 2 CoMFA model was chosen as an alternative in order to establish a starting point for ligand design and lead optimization. While this model is not an ideal screening tool for the new lead compounds, its advantages are (1) close pharmacophoric agreement between the arylsulfonyl isoquinoline compounds used to generate that model and the new ligands, (2) extremely high predictivity as determined by a test set of experimentally analyzed, pharmacophorically similar compounds not within the original training set, and (3) the incorporation of substituent variations distributed over the entire molecule, including the zinc-chelating group, yielding a more generally accurate activity prediction than that of models derived from other training sets that focus on more targeted ligand regions. It must nevertheless be kept in mind that, while the TS 2 model may be adequate to predict lead-series activities in broad brushes (i.e., inactive vs active), the training set from which it is derived is too structurally dissimilar from the thalidomide-based compounds for the model to accurately rank compounds marked as active. Moreover, ring cleavage in the second set of inhibitors (see below) would result in a wide variety of conformational possibilities not within the range of the original CoMFA model. We therefore emphasize that the *in silico* predictions obtained in this study are intended to serve as potential design scaffolds and are subject to validation, optimization, and revision through forthcoming experimental synthesis and binding assays.

The 3D-QSAR models referenced above reveal four key prerequisites for effective inhibitor binding: (1) a strongly hydrophobic group, preferably incorporating an aryl ring and few or no substituents, to fit into the MMP-3 S1' pocket, (2) a flexible or semiflexible ring or long-chain structure capable of engaging in hydrophobic interactions with various S1–S2' residue side chains, including very small hydrophobic substituents and (if possible) hydrophilic substituents directed toward the solvent-exposed top of the MMP-3 binding groove, (3) a sulfonamide moiety placed near the P1' substituent to enhance hydrogen bonding to Leu164 and Ala16, and (4) an effective (preferably hydroxamate or carboxylate) zinc-chelating group.

Docking Thalidomide. We hypothesized that the hydrophobic nature of the phthalimide ring would cause it to occupy the S1' subsite, while the flexible six-membered ring would orient itself toward the S2' region and carbonyls on both rings could replace the sulfonamide as hydrogen-bond acceptors. Two adjacent carbonyls could chelate the catalytic zinc, and the protonated ring nitrogen could serve as a hydrogen-bond donor in place of the hydroxamate NH. Docking the thalidomide molecule into the MMP-3 active site (1SLN.pdb)¹⁸ using the industry-standard FlexX docking package and CScore scoring module⁴⁴ confirmed most of these hypotheses and elucidated the zinc-chelating ability of the two carbonyls (Figure 2). The distance between the glutarimide ring carbonyl oxygen and the catalytic Zn was 2.05 Å, well within the optimal distance of 1.9–2.3 Å; however, the phthalimide carbonyl oxygen was located 2.71 Å from the zinc, indicating a weaker coordination. The flexibility of the six-membered ring probably allows for closer and stronger zinc chelation, whereas the other carbonyl

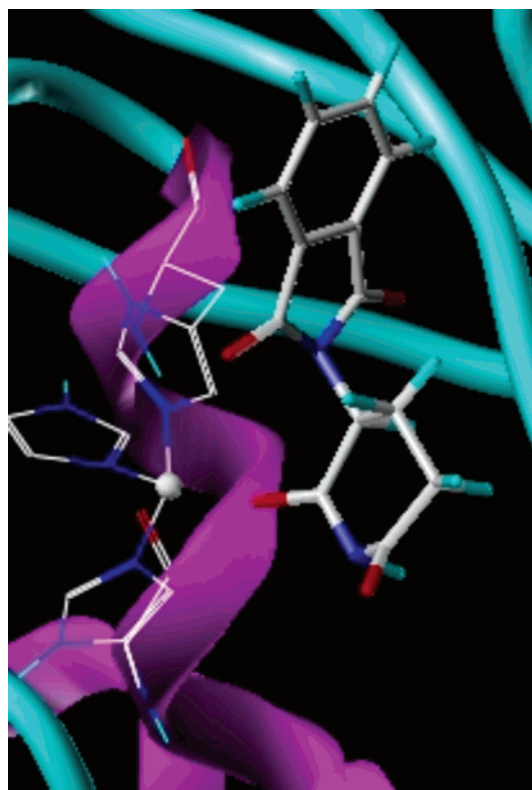


Figure 2. Thalidomide docked into the MMP-3 active site (1SLN.pdb).

is restrained by the more rigid phthalimide group as well as the tight binding of that group to the S1' subsite.

Inhibitor Design. We suspect that the flexibility of the six-membered ring may play a crucial role in the overall binding of thalidomide to MMP-3, affecting hydrophobic and hydrogen-bonding interactions as well as zinc chelation. As elucidated in the 3D-QSAR models derived from TS 3, the conformational changes undergone by the thiazepine rings upon binding suggest that a less rigid structure designed to fit the S1–S2' subsite may enable a greater number of hydrophobic interactions with residues in that region.

The two unsubstituted glutarimide ring carbons appeared to be ideal candidates for the addition of small hydrophobic functional groups as suggested by the CoMFA and CoMSIA analyses. A series of 70 potential MMPIs was constructed by attaching a broad spectrum of functionalities varying in size and polarity to one or both of the unsubstituted carbons on the six-membered ring (Figure 3), generating either one or two chiral centers. Although these structures appeared promising, most were too hydrophobic to be orally available. To guide ligand design, the bioavailability of all compounds was initially assessed by two standard methods: (a) measuring lipophilicity as estimated by the octanol–water partition coefficient ClogP⁴⁵ and (b) screening to satisfy Lipinski's Rule of Five.⁴⁶ The ClogP of the thalidomide molecule itself is fairly low at 0.528; however, the addition of hydrophobic substituents to the unaltered skeleton raised the ClogP to unacceptably high levels (Table 1). (Note that the ClogP calculation does not take stereochemistry into account and considers positions R₁–R₄ to be equivalent in terms of the effect of substitution on overall hydrophobicity or hydrophilicity.) It became evident that an effective MMP inhibitor must combine hydrophobicity, to enable van der Waals

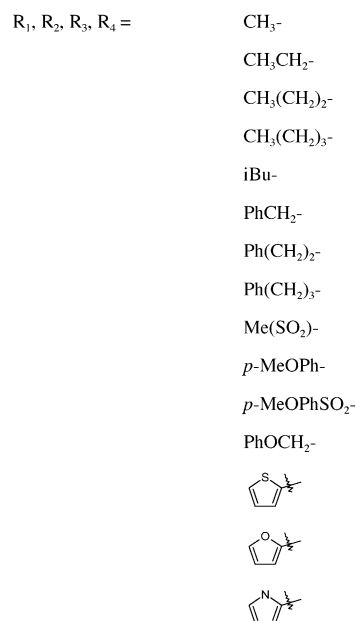
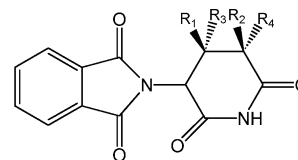


Figure 3. Substitution locations on the thalidomide skeleton.

Table 1. Estimated ClogP Values for Singly-Substituted (R₁–R₄) Thalidomide Molecules (Hydrophobic Substituents)

substituent	estimated ClogP
CH ₃ –	1.047
CH ₃ CH ₂ –	1.576
CH ₃ (CH ₂) ₂ –	2.105
CH ₃ (CH ₂) ₃ –	2.634
<i>i</i> Bu–	2.504
PhCH ₂ –	2.465
Ph(CH ₂) ₂ –	2.994
Ph(CH ₂) ₃ –	3.523

Table 2. Estimated ClogP Values for Singly-Substituted (R₁–R₄) Altered Thalidomide Molecules (Hydrophobic Substituents)

substituent	estimated ClogP
CH ₃ –	0.236
CH ₃ CH ₂ –	0.765
CH ₃ (CH ₂) ₂ –	1.294
CH ₃ (CH ₂) ₃ –	1.823
<i>i</i> Bu–	1.693
PhCH ₂ –	1.654
Ph(CH ₂) ₂ –	2.183
Ph(CH ₂) ₃ –	2.712

interactions with the enzyme side chains, with hydrophilicity to enhance bioavailability. This is not an easy balance to strike, given our findings that MMP ligand binding depends greatly on hydrophobic interactions.

Recent data suggest that an intact glutarimide moiety may not be essential for antimetastatic activity in thalidomide and that thalidomide's antitumor action in fact resides in the phthalimide group.³⁰ We found that altering the phthalimide moiety does not seem to enhance binding affinity in either inhibitor set, regardless of location, which agrees with *in vivo* experimental data obtained on different sets of thalidomide analogues.³⁰ We therefore chose to open the six-

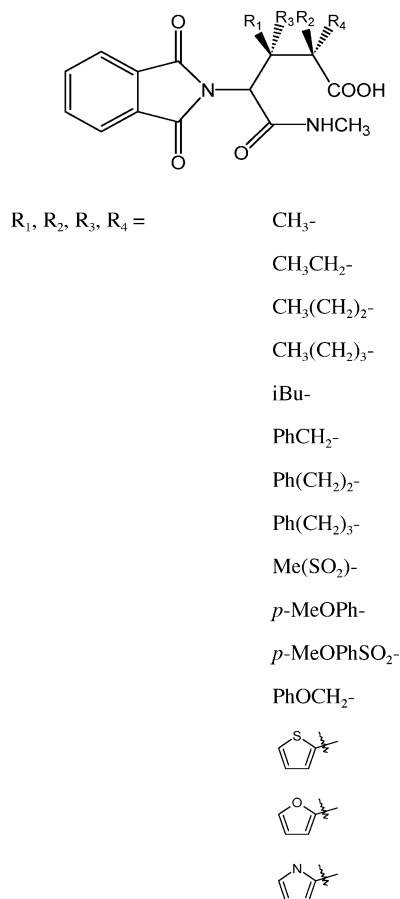


Figure 4. Modified carboxylate-substituted thalidomide skeleton.

membered ring, add a methyl group to the ring nitrogen, and attach a carboxylate moiety to the previously adjacent carbon (Figure 4). These changes rendered the compound too hydrophilic to act as an effective drug on its own (ClogP = -0.163) but allowed the addition of hydrophobic substituents.


uents without driving ClogP too high (Table 2). Opening the glutarimide grouping resulted in even more conformational freedom of the P2' substituents, and the carboxylate moiety could function as an additional hydrogen-bond acceptor. An array of substituents was added to positions R₁–R₄, *a* and *b* to the carboxylate (Figure 4), creating 70 additional potential MMPIs, for a total of 140.

RESULTS AND DISCUSSION

Each potential MMPI was evaluated for potency against MMP-3 by using the most predictive CoMFA model in the present study from the arylsulfonyl isoquinoline TS 2 to assess its biological activity. To prepare for the CoMFA evaluation, the conformation of each novel MMPI was adjusted to match that of the docked thalidomide molecule as closely as possible, and the molecules were aligned to the docked compound in Cartesian space. Gasteiger–Huckel charges were calculated for each molecule to match the charge formalism used in the TS 2 CoMFA model.

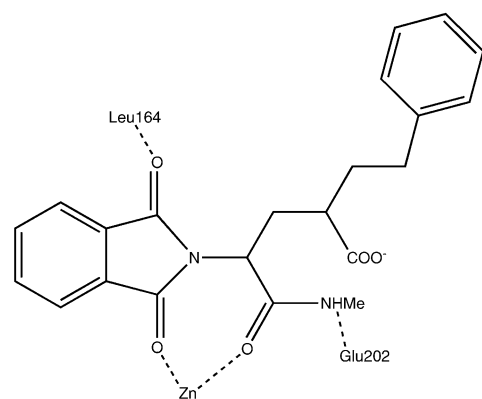
The structures and CoMFA-predicted biological activities of the top 20 novel MMPi are listed in Table 3. Most inhibitors displayed considerable predicted potency against MMP-3, with pIC_{50} values ranging from 6.203 to 9.453. The compounds built on the acidic altered thalidomide structure generally demonstrated higher predicted activity than those built on the intact molecule, possibly because of the increased hydrogen-bonding opportunities described above. The most active inhibitor among both sets was 102, with a predicted pIC_{50} of 9.453 (Figure 5), with compounds 107, 90, and 86 placing second, third, and fourth, respectively. Inhibitor 102 incorporated a fairly large $\text{Ph}(\text{CH}_2)_2-$ group located at the R_4 position; its high activity was initially unexpected because small hydrophobic groups seemed to be favored in that area. The predicted activity of the corresponding compound in the first inhibitor set (intact thalidomide scaffold) was 8.1392, higher than the average for that series but not the highest.

Table 3. CoMFA-Predicted Activities of the Top 20 New MMP-3 Inhibitors

compound	skeleton ^a	R ₁	R ₂	R ₃	R ₄	predicted pIC ₅₀
102	acidic	H—	H—	H—	Ph(CH ₂) ₂ —	9.453
107	acidic	MeSO ₂ —	H—	H—	H—	9.349
90	acidic	H—	H—	H—	<i>n</i> -Bu—	9.310
86	acidic	H—	H—	H—	<i>n</i> -Pr—	9.265
69	intact	<i>p</i> -MeOPhSO ₂ —	H—	H—		9.223
27	intact	H—	H—	PhCH ₂ —	H—	9.170
88	acidic	H—	<i>n</i> -Bu—	H—	H—	9.139
72	acidic	H—	Me—	H—	H—	9.110
13	intact	<i>n</i> -Pr—	H—	H—	H—	9.041
75	acidic	<i>i</i> Bu—	H—	H—	H—	9.013
45	intact	<i>p</i> -MeOPhSO ₂ —	H—	H—	H—	8.821
46	intact	H—	<i>p</i> -MeOPhSO ₂ —	H—	H—	8.780
115	acidic	<i>p</i> -MeOPhSO ₂ —	H—	H—	H—	8.753
25	intact	PhCH ₂ —	H—	H—	H—	8.739
36	intact	H—	H—	H—	Ph(CH ₂) ₃ —	8.731
9	intact	Et—	H—	H—	H—	8.710
50	intact	H—	PhOCH ₂ —	H—	H—	8.632
120	acidic	H—	PhOCH ₂ —	H—	H—	8.624
71	acidic	Me—	H—	H—	H—	8.584
10	intact	H—	Et—	H—	H—	8.581
14	intact	H—	<i>n</i> -Pr	H—	H—	8.544
109	acidic	H—	H—	MeSO ₂ —	H—	8.527
29	intact	Ph(CH ₂) ₂ —	H—	H—	H—	8.474
26	intact	H—	PhCH ₂ —	H—	H—	8.145

^a Intact = built on the unaltered thalidomide skeleton. Acidic = built on the modified carboxylate-substituted thalidomide skeleton.

Phe186, Phe210

pIC₅₀ = 9.453

ClogP = 2.183

Figure 5. Compound 102: inhibitor with highest predicted activity.

The high potency of 102 could be explained by the fact that ring cleavage allows the newly formed four-carbon chain, as well as the large substituent group(s) and terminal carboxylate, to explore a larger region of the MMP-3 binding groove and engage in additional hydrophobic and hydrogen-bonding interactions. The specific steric requirements of the S1–S2' site could then be rendered less important in terms of overall ligand binding.

Docking 102 into the MMP-3 active site elucidated an important hydrophobic interaction between the Ph(CH₂)₂– group and two active-site phenylalanines (Phe186 and Phe210), which also interact with the smaller lipophilic functionalities in 90 and 86. Docking and scoring 102 also revealed a rather unusual MMP-3 binding mode for this class of molecules, with the two carbonyls rather than the carboxylate moiety chelating the catalytic Zn. This was unexpected as the majority of successful MMPi to date incorporate weak acid functionalities that coordinate to the active-site zinc. However, the two carbonyls coordinated quite tightly to the Zn (an improvement upon the unaltered thalidomide structure), and this coordination scheme may have been favored over carboxylate chelation because it enables the adjacent amide nitrogen to form a critical hydrogen bond with Glu202, in effect reproducing hydroxamate Zn chelation.² Compounds 107 and 69 exhibited high predicted activities, with SO₂ moieties in the R₁ position that engage in hydrogen bonding with Leu164 and Ala165, and no strongly hydrophobic functionality at R₄. Overall, hydrogen-bond acceptors are favored at R₁ over the other three modification sites, whereas hydrophobic groups are favored at R₄. Combining a sulfone group at R₁ with a hydrophobic group at R₄, however, resulted in only minimal improvement, most likely because of a disfavored increase in steric bulk distributed over a larger area.

Compound 102 demonstrated an acceptable but slightly high ClogP (2.183) and satisfies Lipinski's Rule of Five. Compounds 90 and 86 had predicted lipophilicities of 1.823 and 1.294, respectively. Adding five-membered rings incorporating heteroatoms to the glutarimide moiety does not enhance binding affinity in either inhibitor set, regardless of location, and appears to have a negative effect on activity in the second (acidic) set, with the notable exception of compound 69.

CONCLUSION

A preliminary in silico series of 140 thalidomide-based matrix metalloproteinase inhibitors was designed with the help of steric, electrostatic, and hydrogen-bonding information obtained from three separately published CoMFA analyses. Substituents were adjusted to accommodate the steric and hydrophobic requirements of the S1–S2' binding area, the characteristics of which were elucidated in our previous work. CoMFA was found to be a highly effective tool for designing, evaluating, and rank-ordering potential MMP inhibitors, providing further information about the MMP-3 binding groove while avoiding the atom-typing problem encountered when applying molecular mechanics techniques to transition metals. Thalidomide, a powerful antineoplastic and antiangiogenic agent, constitutes a convenient starting material for designing and optimizing effective MMPi, in terms of the potential for structural modifications as well as inherent activity. The vast majority of our new preliminary compounds displayed high predicted activity against MMP-3, although the CoMFA model used to predict activity was too structurally dissimilar from the new inhibitors to provide accurate ranking beyond potentially "active" and "inactive". Inhibitors built from the altered thalidomide scaffold, with an opened glutarimide moiety, were generally predicted as more potent than those derived from the unaltered thalidomide molecule. The inhibitors in the second set also exhibited acceptable bioavailability (calculated as ClogP). The compounds with the highest predicted activity from this set show promise as starting points for potential drug candidates. Synthesis, experimental analysis, detailed ADME/Tox-related property prediction, and further optimization of these ligands are to follow.

Supporting Information Available: Structures and CoMFA-predicted biological activity data for all 140 thalidomide-based MMPi. This information is available free of charge via the Internet at <http://pubs.acs.org>.

REFERENCES AND NOTES

- (1) Morgunova, E.; Tuuttila, A.; Bergmann, U.; Isupov, M.; Lindqvist, Y.; Schneider, G.; Tryggvason, K. Structure of human pro-matrix metalloproteinase-2: Activation mechanism revealed. *Science* **1999**, *284*, 1667–1670.
- (2) Whittaker, M.; Floyd, C.; Brown, P.; Gearing, A. Design and therapeutic application of matrix metalloproteinase inhibitors. *Chem. Rev.* **1999**, *99*, 2735–2776.
- (3) Pikul, S.; Dunham, K.; Almstead, N.; De, B.; Natchus, M.; Anastasio, M.; McPhail, S.; Snider, C.; Taiwo, Y.; Chen, L.; Dunaway, C.; Gu, F.; Mieling, G. Design and synthesis of phosphinamide-based hydroxamic acids as inhibitors of matrix metalloproteinases. *J. Med. Chem.* **1999**, *42*, 87–94.
- (4) Fichter, M.; Korner, U.; Schomburg, J.; Jennings, L.; Cole, A.; Mollenhauer, J. Collagen degradation products modulate matrix metalloproteinase expression in cultured articular chondrocytes. *J. Orthop. Res.* **2006**, *24*, 63–70.
- (5) Kanesaka, T.; Mori, M.; Hattori, T.; Oki, T.; Kuwabara, S. Serum matrix metalloproteinase-3 levels correlate with disease activity in relapsing-remitting multiple sclerosis. *J. Neurol. Neurosurg. Psychiatry* **2006**, *77*, 185–188.
- (6) Evio, S.; Tarkkila, L.; Sorsa, T.; Furuholm, J.; Valimaki, M.; Ylikorkala, O.; Tiitinen, A.; Meurman, J. Effects of alendronate and hormone replacement therapy, alone and in combination, on saliva, periodontal conditions and gingival crevicular fluid matrix metalloproteinase-8 levels in women with osteoporosis. *Oral Dis.* **2006**, *12*, 187–193.
- (7) Mendes, O.; Kim, H.; Stoica, G. Expression of MMP2, MMP9 and MMP3 in breast cancer brain metastasis in a rat model. *Clin. Exp. Metastasis* **2005**, *22*, 237–246.

- (8) Bachmeier, B.; Albin, A.; Vene, R.; Benelli, R.; Noonan, D.; Weigert, C.; Weiler, C.; Lichtinghagen, R.; Jochum, M.; Nerlich, A. Cell density-dependent regulation of matrix metalloproteinase and TIMP expression in differently tumorigenic breast cancer cell lines. *Exp. Cell. Res.* **2005**, *305*, 83–98.
- (9) Malesud, C. Matrix metalloproteinases (MMPs) in health and disease: An overview. *Front. Biosci.* **2006**, *11*, 1696–1701.
- (10) Bokarewa, M.; Dahlberg, L.; Tarkowski, A. Expression and functional properties of antibodies to tissue inhibitors of metalloproteinases (TIMPs) in rheumatoid arthritis. *Arthritis Res. Ther.* **2005**, *7*, 1014–1022.
- (11) Lohmander, L.; Brandt, K.; Mazzuca, S.; Katz, B.; Larsson, S.; Struglics, A.; Lane, K. Use of the plasma stromelysin (matrix metalloproteinase 3) concentration to predict joint space narrowing in knee osteoarthritis. *Arthritis Rheum.* **2005**, *52*, 3160–3167.
- (12) Li, M.; Yamamoto, H.; Adachi, Y.; Maruyama, Y.; Shinomura, Y. Role of matrix metalloproteinase-7 (matrilysin) in human cancer invasion, apoptosis, growth, and angiogenesis. *Exp. Biol. Med.* **2006**, *231*, 20–27.
- (13) Przybylowska, K.; Klucznak, A.; Zadrozny, M.; Krawczyk, T.; Kulig, A.; Rykala, J.; Kolacinska, A.; Morawiec, Z.; Drzewoski, J.; Blasiak, J. Polymorphisms of the promoter regions of matrix metalloproteinases genes MMP-1 and MMP-9 in breast cancer. *Breast Cancer Res. Treat.* **2006**, *95*, 65–72.
- (14) Vihinen, P.; Ala-aho, R.; Kahari, V. Matrix metalloproteinases as therapeutic targets in cancer. *Curr. Cancer Drug Targets* **2005**, *5*, 203–220.
- (15) Chen, X.; Su, Y.; Fingleton, B.; Acuff, H.; Matrisian, L.; Zent, R.; Pozzi, A. Increased plasma MMP9 in integrin $\alpha 1$ -null mice enhances lung metastasis of colon carcinoma cells. *Int. J. Cancer* **2005**, *116*, 52–61.
- (16) Tas, F.; Duranyildiz, D.; Oguz, H.; Disci, R.; Kurul, S.; Yasasever, V.; Topuz, E. Serum matrix metalloproteinase-3 and tissue inhibitor of metalloproteinase-1 in patients with malignant melanoma. *Med. Oncol. (Totowa, NJ, U.S.)* **2005**, *22*, 39–44.
- (17) Kerkela, E.; Saarialho-Kere, U. Matrix metalloproteinases in tumor progression: Focus on basal and squamous cell skin cancer. *Exp. Dermatol.* **2003**, *12*, 109–125.
- (18) Becker, J.; Marcy, A.; Rokosz, L.; Axel, M.; Burbaum, J.; Fitzgerald, P.; Cameron, P.; Esser, C.; Hagmann, W.; Hermes, J.; Springer, J. Stromelysin-1: Three-dimensional structure of the inhibited catalytic domain and of the C-truncated proenzyme. *Protein Sci.* **1995**, *4*, 1966–1976.
- (19) Gooley, P.; O'Connell, J.; Marcy, A.; Cuca, G.; Axel, M.; Caldwell, C.; Hagmann, W.; Becker, J. Comparison of the structure of human recombinant short form stromelysin by multidimensional heteronuclear NMR and X-ray crystallography. *J. Biomol. NMR* **1996**, *7*, 8–28.
- (20) Corral, L. G.; Kaplan, G.; Stirling, D.; Wu, M.; Chen, Y.; Moreira, A.; Muller, G. Selection of novel analogs of thalidomide with enhanced tumor necrosis factor- α inhibitory activity. *Mol. Med.* **1996**, *2*, 506–515.
- (21) Minchinton, A.; Fryer, K.; Wendt, K.; Clow, K.; Hayes, M. The effect of thalidomide on experimental tumors and metastases. *Anti-Cancer Drugs* **1996**, *7*, 339–343.
- (22) Kling, J. Redeeming thalidomide. *Modern Drug Discovery* **2000**, June, 35–39.
- (23) Grover, J.; Vats, V.; Gopalakrishna, R.; Ramam, M. Thalidomide: A re-look. *Natl. Med. J. India* **2000**, *13*, 132–141.
- (24) Teo, S.; Stirling, D.; Zeldis, J. Thalidomide as a novel therapeutic agent: new uses for an old product. *Drug Discovery Today* **2005**, *10*, 107–114.
- (25) Moreira, A.; Kaplan, G.; Villahermosa, L.; Fajardo, T.; Abalos, R.; Cellona, R.; Balagon, M. Comparison of pentoxifylline, thalidomide and prednisone in the treatment of ENL. *Int. J. Lepr. Other Mycobact. Dis.* **1998**, *66*, 61–65.
- (26) Shimazawa, R.; Miyachi, H.; Takayama, H.; Kuroda, K.; Kato, F.; Kato, M.; Hashimoto, Y. Antiangiogenic activity of tumor necrosis factor- α production regulators derived from thalidomide. *Biol. Pharm. Bull.* **1999**, *22*, 224–226.
- (27) Folkman, J.; Browder, T.; Palmblad, J. Angiogenesis research: Guidelines for translation to clinical application. *Thromb. Haemostasis* **2001**, *86*, 23–33.
- (28) D'Amato, R.; Loughnan, M.; Flynn, E.; Folkman, J. Thalidomide is an inhibitor of angiogenesis. *Proc. Natl. Acad. Sci. U.S.A.* **1994**, *91*, 4082–4085.
- (29) Knight, R. IMiDs: A novel class of immunomodulators. *Semin. Oncol.* **2005**, *32*, S24–30.
- (30) Shah, J.; Swartz, G.; Papathanassiou, A.; Treston, A.; Fogler, W.; Madsen, J.; Green, S. Synthesis and enantiomeric separation of 2-phthalimidino-glutaric acid analogues: Potent inhibitors of tumor metastasis. *J. Med. Chem.* **1999**, *42*, 3014–3017.
- (31) Muller, G.; Corral, L.; Shire, M.; Wang, H.; Moreira, A.; Kaplan, G.; Stirling, D. Structural modifications of thalidomide produce analogs with enhanced tumor necrosis factor inhibitory activity. *J. Med. Chem.* **1996**, *39*, 3238–3240.
- (32) SYBYL, 6.7; SYBYL, 7.0; Tripos, Inc., St. Louis, MO.
- (33) Cramer, R.; Patterson, D.; Bunce, J. Effect of shape on binding of steroids to carrier proteins. *J. Am. Chem. Soc.* **1988**, *110*, 5959–5967.
- (34) Klebe, G.; Abraham, U.; Mietzner, T. Molecular similarity indices in a comparative analysis (CoMSIA) of drug molecules to correlate and predict their biological activity. *J. Med. Chem.* **1994**, *37*, 4130–4146.
- (35) Cheng, M.; De, B.; Pikul, S.; Almstead, N.; Natchus, M.; Anastasio, M.; McPhail, S.; Snider, C.; Taiwo, Y.; Chen, L.; Dunaway, C.; Gu, F.; Dowty, M.; Mieling, G.; Janusz, M.; Wang-Weigand, S. Design and synthesis of piperazine-based matrix metalloproteinase inhibitors. *J. Med. Chem.* **2000**, *43*, 369–380.
- (36) Matter, H.; Schwab, W. Affinity and selectivity of matrix metalloproteinase inhibitors: A chemometrical study from the perspective of ligands and proteins. *J. Med. Chem.* **1999**, *42*, 4506–4523.
- (37) Almstead, N.; Bradley, R.; Pikul, S.; De, B.; Natchus, M.; Taiwo, Y.; Gu, F.; Williams, L.; Hynd, B.; Janusz, M.; Dunaway, C.; Mieling, G. Design, synthesis, and biological evaluation of potent thiazine- and thiazepine-based matrix metalloproteinase inhibitors. *J. Med. Chem.* **1999**, *42*, 4547–4562.
- (38) Amin, E.; Welsh, W. Three-dimensional quantitative structure–activity relationship (3D-QSAR) models for a novel class of piperazine-based stromelysin-1 (MMP-3) inhibitors: Applying a “divide and conquer” strategy. *J. Med. Chem.* **2001**, *44*, 3849–3855.
- (39) Amin, E.; Welsh, W. Forthcoming.
- (40) Matter, H.; Schwab, W.; Barbier, D.; Billen, G.; Haase, B.; Neises, B.; Schudok, M.; Thorwart, W.; Schreuder, H.; Brachvogel, V.; Lonze, P.; Weithmann, K. Quantitative structure–activity relationship of human neutrophil collagenase (MMP-8) inhibitors using comparative molecular field analysis and X-ray structure analysis. *J. Med. Chem.* **1999**, *42*, 1908–1920.
- (41) Kunick, C.; Laurenroth, K.; Wiekling, K.; Zie, X.; Schultz, C.; Gussio, R.; Zaharevitz, D.; Leost, M.; Meijer, L.; Weber, A.; Jorgensen, F.; Lemcke, T. Evaluation and comparison of 3D-QSAR CoMSIA models for CDK1, CDK5, and GSK-3 inhibition by paullones. *J. Med. Chem.* **2004**, *47*, 22–36.
- (42) Paula, S.; Tabet, M.; Keenan, S.; Welsh, W.; Ball, W. Three-dimensional structure–activity relationship modeling of cocaine binding to two monoclonal antibodies. *J. Mol. Biol.* **2003**, *325*, 515–530.
- (43) Johnson, T.; Khan, I.; Avery, M.; Grant, J.; Meshnick, S. Quantitative structure–activity relationship studies of a series of sulfa drugs as inhibitors of *Pneumocystis carinii* dihydropteroate synthetase. *Anti-microb. Agents Chemother.* **1998**, *42*, 1454–1458.
- (44) Rarey, M.; Kramer, B.; Lengauer, T. Multiple automatic base selection: Protein–ligand docking based on incremental construction without manual intervention. *J. Comput.-Aided Mol. Des.* **1997**, *11*, 369.
- (45) Veber, D.; Johnson, S.; Cheng, H.; Smith, B.; Ward, K.; Kopple, K. Molecular properties that influence the oral bioavailability of drug candidates. *J. Med. Chem.* **2002**, *45*, 2615–2623.
- (46) Lipinski, C.; Lombardo, F.; Dominy, B.; Feeney, P. Experimental and computational approaches to estimate solubility and permeability in drug discovery and development settings. *Adv. Drug Delivery Rev.* **1997**, *23*, 3–25.

CI0601362